J|A|C|S
COMMUNICATIONS

Published on Web 01/23/2007

Chemical Transformation from FePt to $Fe_{1-x}PtM_x$ (M = Ru, Ni, Sn) Nanocrystals by a Cation Redox Reaction: X-ray Absorption Spectroscopic Studies

Di-Yan Wang,[†] Ching-Hsiang Chen,[‡,||] Hung-Chi Yen,[†] You-Liang Lin,[†] Pei-Yu Huang,[†] Bing-Joe Hwang,*[,‡,§] and Chia-Chun Chen*[,†,||]

Department of Chemistry, National Taiwan Normal University, Taipei 116, Taiwan, Nanoelectrochemistry Laboratory, Department of Chemical Engineering, National Taiwan University of Science and Technology, Taipei 106, Taiwan, National Synchrotron Radiation Research Center (NSRRC), Hsinchu 300, Taiwan, R.O.C., and Institute of Atomic and Molecular Sciences, Academia Sinica, Taipei 115, Taiwan

Received October 31, 2006; E-mail: cjchen@ntnu.edu.tw

Recent, new synthetic approaches have been intensively explored to prepare new types of nanostructures using a chemical replacement reaction in a solution phase.[1,2] The crystal compositions, structures, and shapes of starting nanocrystals might have been varied after they were chemically transformed into new types of nanostructures. For example, the studies on silver nanocrystals in the presence of gold ions have shown that the replacement reaction resulted in the product of gold nanocrystals with a significant shape transformation.[1a,2c] The driving force of this specific reaction of the nanocrystals was attributed to the differences of the reduction potentials between silver and gold. Several other examples have also demonstrated that the new types of metal nanostructures, such as hollow,[1] core/shell nanocrystals,[3] or nanocrystal dimers,[4] were formed under different reaction conditions. Besides the chemical replacement reaction between two pure metals, the binary semiconductor CdSe nanocrystals were transformed reversibly into Ag_2Se nanocrystals by a cation-exchange reaction.[5] These examples have suggested that the chemical replacement or galvanic reduction−oxidation (redox) reaction of nanocrystals might be a quite useful method to apply for the preparation of other new types of nanostructures.

The PtRu nanocrystals have been intensively investigated recently because of their unique catalytic properties for fuel cell applications.[6,7] One always looks for new types of metal nanocrystals with improved catalytic performance to replace expensive Pt and Ru metals for commercial purposes.[8] In this report, we selected FePt nanocrystals and the metal ions, M^{n+} = Ru^{3+}, Sn^{2+}, or Ni^{2+}, as reactants to produce new ternary metal nanocrystals of $Fe_{1-x}PtM_x$ using a cation-redox reaction in a solution (Figure 1). The structure and composition of resulting nanocrystals were characterized by transmission electron microscopy (TEM), X-ray diffraction (XRD), and X-ray photoemission spectroscopy (XPS). Moreover, X-ray absorption near-edge spectroscopy (XANES) was employed to confirm the chemical transformation from FePt to $Fe_{1-x}PtRu_x$ nanocrystals. The analyses of extended X-ray absorption find structure (EXAFS) revealed the detailed binding structures and coordination numbers of both FePt and $Fe_{1-x}PtRu_x$ nanocrystals. The results suggested that iron atoms of FePt lattices were oxidized to be Fe^{2+} and Fe^{3+} ions and were replaced by ruthenium atoms from the reduction of Ru^{3+} ions in solution to form $Fe_{1-x}PtRu_x$ lattices. Our method has opened a new route to easily and rapidly prepare a solid-solution type of ternary metal nanocrystals for catalytic applications.

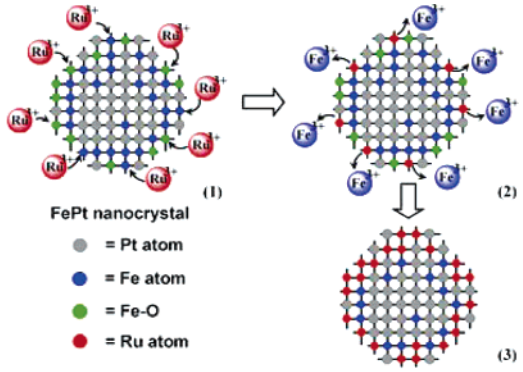

Figure 1. Schematic illustration of chemical transformation from FePt to $Fe_{1-x}PtRu_x$ nanocrystals in solution. (1) Ru^{3+} ions and FePt nanocrystals were mixed in the solution. (2) Then, the cation redox reaction occurs between Ru^{3+} ions and the Fe species including Fe atoms of FePt nanocrystals and a small amount of FeO on the nanocrystal surface. The ions of Fe^{2+} and Fe^{3+} were gradually formed in the solution, and Ru^{3+} ions were reduced to Ru atoms in the FePt lattices. (3) Finally, the ternary $Fe_{1-x}PtRu_x$ nanocrystals were produced

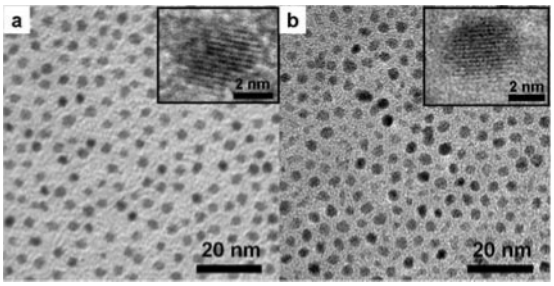

Figure 2. High-resolution TEM images of (a) FePt and (b) $Fe_{1-x}PtRu_x$ nanocrystals. The averaged sizes of the nanocrystals are calculated to be ~4 nm for both samples. The lattice fringes of the samples were observed clearly (insets of upper corner) in the images, showing that the crystal structures were well maintained after the cation redox reaction.

The starting materials, FePt nanocrystals, were synthesized by following the previous report with some modifications.[9] High-resolution TEM images of resulting FePt nanocrystals in Figure 2a have shown that the nanocrystals were crystalline with clear lattice structures. The nanocrystals were uniform and well-dispersed on the TEM grid with an average diameter of ~4 nm. Energy dispersive X-ray spectroscopy (EDS) of FePt nanocrystals indicated that the ratio of Fe and Pt was approximately 1/1. The XPS results were used to further confirm the compositions and oxidation states of both Fe and Pt of FePt nanocrystals. The solution of FePt nanocrystals was then reacted with the metal ions (M^{n+} = Ru^{3+},

[†] National Taiwan Normal University.
[‡] National Taiwan University of Science and Technology.
[§] National Synchrotron Radiation Research Center (NSRRC).
[||] Institute of Atomic and Molecular Sciences, Academia Sinica.

10.1021/ja067567l CCC: $37.00

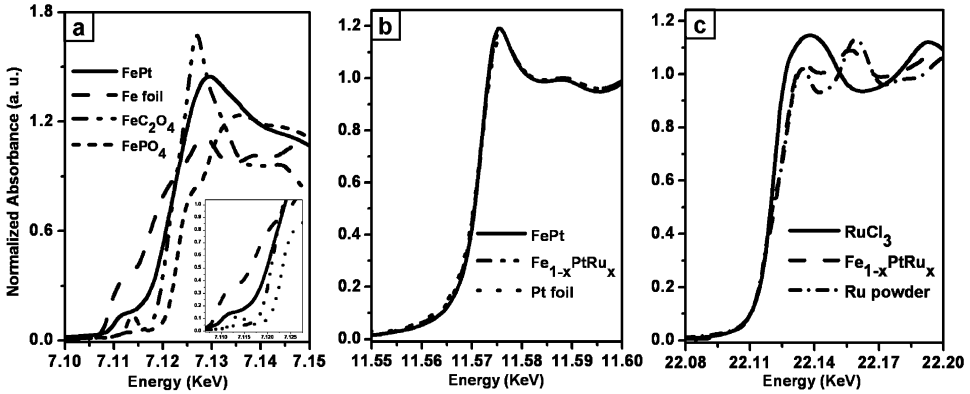

Figure 3. Normalized XANES spectra near the (a) Fe K-edge of FePt nanocrystals and references and in the preedge spectra (inset); (b) Pt L_{III}-edge of FePt, $Fe_{1-x}PtRu_x$ nanocrystals, and Pt foil; and (c) Ru K-edge of $Fe_{1-x}PtRu_x$ nanocrystals, $RuCl_3$, and Ru powder.

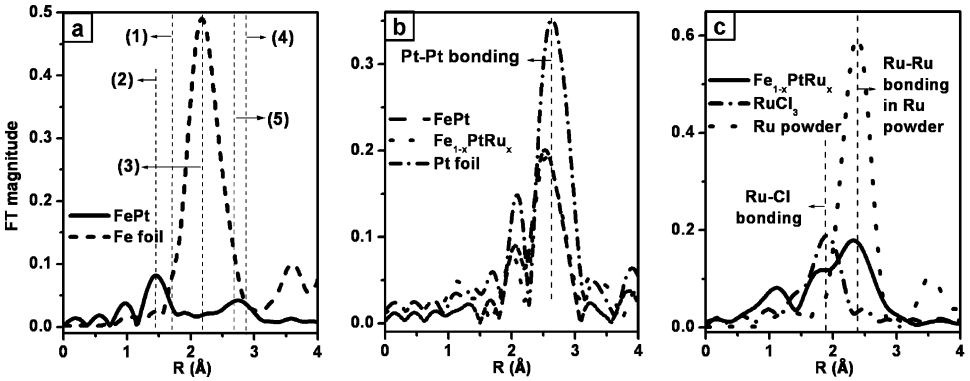

Figure 4. FT-EXAFS spectra at the (a) Fe K-edge of FePt nanocrystals and Fe foil, and the bond distances of (1), (2), (3), (4), (5) are Fe−Cl bonding, Fe−O bonding in Fe−O, Fe−Fe bonding in Fe metal, Fe−Fe bonding in Fe−O, and Fe−Pt bonding, repectively; (b) Pt L_{III}-edge of FePt, $Fe_{1-x}PtRu_x$ nanocrystals, and Pt foil; and (c) Ru K-edge of $Fe_{1-x}PtRu_x$ nanocrystals, $RuCl_3$, and Ru powder.

Sn^{2+}, or Ni^{2+}) at 85 °C. The redox reaction between FePt nanocrystals and the metal ions was monitored qualitatively by detecting the release of Fe^{2+} and Fe^{3+} ions using 1,10-phenanthroline or thiocyanate anions as an indicator in the solution. A clear color change of the solutions with the indicator was readily observed, suggesting that Fe elements of FePt nanocrystals were oxidized to be Fe^{2+} and Fe^{3+} ions. No color change was found in the control experiment when Ru^{3+}, Sn^{2+}, or Ni^{2+} was not added into FePt nanocrystal solution. The typical TEM image (Figure 2b) of the resulting $Fe_{1-x}PtM_x$ nanocrystals revealed that there was no significant change on the average size and shape of $Fe_{1-x}PtM_x$ nanocrystals in comparison to those of original FePt nanocrystals (Figure 2a). The nanocrystals kept similar crystal structures and average sizes (calculated by Scherrer's equation) before and after the chemical transformation based on the X-ray and electron diffraction measurements. The compositions of $Fe_{1-x}PtM_x$ nanocrystals were further confirmed by EDS, XPS, XANES, and EXAFS. Typically under the reaction time of 1 h, the Fe/Ru ratio of resulting $Fe_{1-x}PtRu_x$ nanocrystals is calculated from X-ray absorption spectroscopy (XAS) by measuring the edge jump ($\Delta\mu\chi$),[10] and it showed that the ratio of Fe/Ru is 0.27/0.73.[11] The overall results suggested that metal ions, M^{n+}, were indeed reduced to be metal atoms of $Fe_{1-x}PtM_x$ nanocrystals, and iron atoms of FePt nanocrystals were oxidized and released as Fe^{2+} and Fe^{3+} in the solution.

To further understand the details of the redox reaction of the FePt nanocrystals and the metal ions, X-ray absorption spectroscopy using a synchrotron radiation source was performed on the samples of FePt and $Fe_{1-x}PtRu_x$ nanocrystals. The Fe K-edge XANES spectra of the bimetallic FePt powder and reference compounds (Fe foil, FeC_2O_4, and $FePO_4$) are shown in Figure 3a. The edge energy position of the FePt sample is found to be between that of the reference compounds of Fe foil and FeC_2O_4, indicating that the iron element in FePt nanocrystals is a mixture of Fe^0 and Fe^{2+}. Figure 3b shows that the white line feature of FePt and $Fe_{1-x}PtRu_x$ samples is the same as that of Pt foil, implying that the oxidation state of Pt in the FePt and $Fe_{1-x}PtRu_x$ nanocrystals remained Pt^0. The composition of iron in the sample $Fe_{1-x}PtRu_x$ is too low to get EXAFS spectra of good resolution at Fe K-edge, indicating that a large number of the Fe atoms have been replaced by the Ru atoms. However, Ru elements can be observed at Ru K-edge for the $Fe_{1-x}PtRu_x$ sample. The XANES feature of Ru K-edge for the $Fe_{1-x}PtRu_x$ nanocrystals is close to that for Ru powders as shown in Figure 3c, indicating that most of the Ru species have been reduced to the Ru^0 state. It is suggested that the Fe atoms in the bimetallic nanocrystals can react with Ru^{3+} via chemical transformation. The electrons required for the reduction of Ru^{3+} ions are contributed from the oxidation of Fe^0 to Fe^{3+} or Fe^{2+} to Fe^{3+}.

Figure 4 shows the Fourier transformed k^3-weighted EXAFS spectra of the FePt and $Fe_{1-x}PtRu_x$ nanocrystals. The structural parameters extracted from the EXAFS spectra for the samples of FePt and $Fe_{1-x}PtRu_x$ powders in nanocrystals are listed in Table 1, in which the fittings were based on the fcc structure and the FeO crystal structure, respectively, using the FEFF7 software package.[12,13] The spectrum of the Fe K-edge of the FePt nanocrystals (Figure 4a) demonstrates a peak between 1.3 and 2.0 Å corresponding to the Fe−O bond as confirmed by FEFF7 fitting based on the FeO structure. If the iron atoms are occupied in the core region, the iron would not be oxidized to form the FeO species because the oxygen from air would not quickly diffuse into the

Table 1. Structural Parameters[a] Derived from the Fe K-edge, Pt L_{III}-edge, and Ru

edge	shell	N	R_j (Å)	σ^2(×10^{-3}) (Å^2)	ΔE_0 (eV)
		FePt			
Fe	Fe−O	3.2	1.899	5.0	−18.0
K-edge	Fe−Pt	5.6	2.683	7.9	2.7
	Fe−Fe	3.8	3.190	0.0	13.7
Pt	Pt−Fe	1.7	2.683	7.2	3.9
L_{III}-edge	Pt−Pt	6.8	2.736	6.0	4.1
		$Fe_{1-x}PtRu_x$			
Pt	Pt−Fe	0.4	2.724	0.0	3.9
L_{III}-edge	Pt−Pt	6.8	2.736	6.2	3.8
Ru	Ru−Cl	2.7	2.347	0.0	17.3
K-edge	Ru−Fe	1.2	2.573	8.0	12.2
	Ru−Ru	3.3	2.717	0.0	−13.6

[a] N: coordination number, R_j: bonding distance, σ^2: Debye−Waller factor, ΔE_0: inner potential shift.

core of the nanocrystals. It is believed that the FeO species would be dispersed on the surface of the FePt nanocrystals. The spectrum also shows a broad peak between 2.0 and 3.3 Å corresponding to the co-oscillation feature of the Fe−Pt bond and Fe−Fe bond. The EXAFS spectra at the Pt L_{III}-edge of the FePt and $Fe_{1-x}PtRu_x$ nanocrystals are shown in Figure 4b. A peak between 1.9 and 3.1 Å corresponding to the Pt−Pt bond of both FePt and $Fe_{1-x}PtRu_x$ samples is shorter than that of Pt foil, indicating that the heteroatomic bonding exists in the Pt core atoms of both the FePt and $Fe_{1-x}PtRu_x$ samples. As shown in Table 1, the coordination number of N_{Pt-Fe} and N_{Pt-Pt} is found to be 1.7 and 6.8 for the FePt nanocrystals and 0.4 and 6.8 for the $Fe_{1-x}PtRu_x$ nanocrystals, respectively. The coordination number of N_{Pt-Fe} is decreased from 1.7 in the FePt sample to 0.4 in the $Fe_{1-x}PtRu_x$ sample, implying that the most of iron atoms are dissolved after the addition of $RuCl_3$ reactants. It is consistent with the observation of the XANES spectra. The total coordination number of metallic Fe atoms (5.6) is much smaller than that of metallic Pt atoms (8.5) in the case of FePt, indicating that the Pt atoms and Fe atoms are rich in the core region and in shell region, respectively, in the nanocrystals.[7] For the structural model of the FePt nanocrystals, the overall results suggest that most of the Pt atoms are preferentially located in the core region, the Fe atoms are preferentially located in the shell region, and small amounts of the FeO species are dispersed on the surface on the FePt nanocrystals. For $P_{core}-R_{shell}$ nanocrystal model, if all the P atoms are occupied in the core region, the total coordination number of P core atoms should be 12 based on the fcc structure. However, the total coordination number of Pt atoms is 8.5 and 7.2 for the FePt and $Fe_{1-x}PtRu_x$ nanocrystals, respectively, indicating that some of surface sites are occupied by Pt atoms in the shell regions for both samples. Figure 4c shows the Fourier transformed k^3-weighted EXAFS spectra at the Ru K-edge of the $Fe_{1-x}PtRu_x$ nanocrystals. The feature of Fourier transform of $Fe_{1-x}PtRu_x$ nanocrystals at the Ru K-edge shows two peaks between 1.3 and 3.1 Å corresponding to Ru−Cl and Ru−Ru bonds as compared with the reference compounds $RuCl_3$ and Ru powder. The peak position of the Ru−Ru bond is slightly shorter than that of Ru powder, indicating that heteroatomic bonding exists around Ru. The fitting result shows that the coordination numbers of Cl, Fe, and Ru around Ru are found to be 2.7, 1.2, and 3.3, respectively. In our understanding, the Cl coordination would be attributed to the residue of $RuCl_3$ after the galvanic redox reaction. Both the coordination number of Pt around the Ru atoms and the coordination number of Ru around the Pt atoms cannot be extracted and only show the Pt−Fe and Ru−Fe bonds, indicating a three-stacking region in the $Fe_{1-x}PtRu_x$ nanocrystals (Ru−Fe/Fe/Fe−Pt). For the structural model of $Fe_{1-x}PtRu_x$ nanocrystals, these observations indicate that most of the Pt atoms are preferentially located in the core region and the Ru atoms are located in the shell region with a intermediate iron layer between the Pt and Ru atoms.

The new ternary $Fe_{1-x}PtM_x$ nanocrystals were tested for their catalytic properties in the anodic electrode of a fuel cell. Their catalytic capability will be discussed elsewhere. Furthermore, the in situ studies of detailed chemical transformation from binary to ternary metal nanocrystals using X-ray absorption spectroscopy are in progress. Overall, our results have demonstrated a simple and rapid route for the syntheses of new catalysts based on metal alloy nanocrystals.

Acknowledgment. We gratefully thank NSTPNN, NSC, NTNU, NTUST, IAMS, and National Synchrotron Radiation Research Center for financial support for this project.

Supporting Information Available: Experimental procedures, qualitative analysis, XPS, TEM, ED, EDS, and XRD. This material is available free of charge via the Internet at http://pubs.acs.org.

References

(1) (a)Yin, Y.; Erdonmez, C.; Aloni, S.; Alivisatos, A. P. *J. Am. Chem. Soc.* **2006**, *128*, 12671−12673. (b) Yin, Y.; Rioux, R. M.; Erdonmez, C. K.; Hughes, S.; Somorjai, G. A.; Alivisatos, A. P. *Science* **2004**, *304*, 711−714.
(2) (a) Chen, J.; Wiley, B.; McLellan, J.; Xiong, Y.; Li, Z.-Y.; Xia, Y. *Nano Lett.* **2005**, *5*, 2058−2062. (b) Cable, R. E.; Schaak, R. E. *J. Am. Chem. Soc.* **2006**, *128*, 9588−5989. (c) Sun, Y.; Xia, Y. *J. Am. Chem. Soc.* **2004**, *126*, 3892−3901.
(3) (a) Leonard, B. M.; Schaak, R. E. *J. Am. Chem. Soc.* **2006**, *128*, 11475−11482. (b) Lee, W.-R.; Kim, M. G.; Choi, J.-R.; Park, J.-I.; Ko, S. J.; Oh, S. J.; Cheon, J. *J. Am. Chem. Soc.* **2005**, *127*, 16090−16097.
(4) (a) Gu, H. W.; Yang, Z. M.; Gao, J. H.; Chang, C. K.; Xu, B. *J. Am. Chem. Soc.* **2005**, *127*, 34−35. (b) Shi, W. L.; Zeng, H.; Sahoo, Y.; Ohulchanskyy, T. Y.; Ding, Y.; Wang, Z. L.; Swihart, M.; Prasad, P. N. *Nano Lett.* **2006**, *6*, 875−881. (c) Pellegrino, T.; Fiore, A.; Carlino, E.; Giannini, C.; Cozzoli, P. D.; Ciccarella, G.; Respaud, M.; Palmirotta, L.; Cingolani, R.; Manna, L. *J. Am. Chem. Soc.* **2006**, *128*, 6690−6698.
(5) (a) Son, D. H.; Hughes, S. M.; Yin, Y. D.; Alivisatos, A. P. *Science* **2004**, *306*, 1009−1012. (b) Jeong, U.; Kim, J.-U.; Xia, Y.; Li, Z.-Y. *Nano Lett.* **2005**, *5*, 937−942.
(6) Russell, A. E.; Rose, A. *Chem. Rev.* **2004**, *104*, 4613−4635.
(7) Hwang, B. J.; Sarma, L. S.; Chen, J. M.; Chen, C. H.; Shih, S. C.; Wang, G. R.; Liu, D. G.; Lee, J. F.; Tang, M. T. *J. Am. Chem. Soc.* **2005**, *127*, 11140−11145.
(8) (a) Bock, C.; Paquet, C.; Couillard, M.; Botton, G. A.; MacDougall, B. R. *J. Am. Chem. Soc.* **2004**, *126*, 8028−8037. (b) Liao, S.; Holmes, K.-A.; Tsaprailis, H.; Birss, V. I. *J. Am. Chem. Soc.* **2006**, *128*, 3504−3505.
(9) Sun, S. H.; Murray, C. B.; Weller, D.; Folks, L.; Moser, A. *Science* **2000**, *287*, 1989−1992.
(10) Chen, C.-H.; Hwang, B.-J.; Wang, G.-R.; Sarma, L. S.; Tang, M.-T.; Liu, D.-G.; Lee, J.-F. *J. Phys. Chem. B* **2005**, *109*, 21566−21575.
(11) Reactions of FePt nanocrystals with M^{n+} ions were performed under 5 min, and 0.5, 1, 2, and 3 h. All the samples were currently characterized in details by X-ray absorption spectroscopy using a synchrotron source. The data for $Fe_{1-x}PtRu_x$ nanocrystal samples showed that Fe atoms were gradually replaced by Ru atoms, depending on the reaction time. Eventually, PtRu nanocrystals were obtained. More detailed spectroscopic studies on those samples will be discussed elsewhere.
(12) Stern, E. A.; Newville, M.; Ravel, B.; Yacoby, Y.; Haskel, D. *Physica B* **1995**, *208−209*, 117−120.
(13) Zabinsky, S. I.; Rehr, J. J.; Anukodinov, A. L.; Albers, R. C.; Eller, M. *J. Phys. Rev. B* **1995**, *52*, 2995−3009.

JA067567L